Egyptian Journal of Phytopathology, Vol. 53, No.2, pp 111 - 130 (2025)
DOI: 10.21608/EJP.2025.400339.1148

ORIGINAL ARTICLE

Chitosan Nanoparticles Improved Lucky Bamboo Immunity Against *Rhizoctonia solani* and Induced Expression of Defense-Related Genes

Mahmoud M.A.[1], **Al-Morsy S.A**[1], **Ahmed H.F.A.** [1] **Abd El-Aziz A.R.M.**[1]

Received: 3 July 2025 / **Accepted**: 31 August 2025 / **Published online**: 15 September 2025

ABSTRACT

Root rot disease of lucky bamboo leads to economic losses and crop production constraints. Research indicated that chitosan nanoparticles (CH NPs) is an eco-friendly agent for root rot management and reveals potential molecular mechanisms against the pathogen. CH NPs underwent chemical characterization using spectroscopic and microscopic methods including UV-visible spectrophotometry (UV-vis), and transmission electron microscopy (TEM). Following CH NPs confirmation, they were evaluated for antifungal properties and impacts on lucky bamboo's chemical and molecular composition. A survey performed during August–October 2023 across three Egyptian governorates revealed root rot and basal stem rot disease symptoms in lucky bamboo specimens. Maximum disease infection percentage was occurred in lucky bamboo collected from Giza Governorate. Six fungal species belonging to four distinct genera were isolated from lucky bamboo samples, with *Rhizoctonia solani* (*R. solani*) being the most common. CH NPs exhibited potent concentration-dependent fungistatic effects on *R. solani* and substantially decreased mycelial radial development (up to 100% growth inhibition), disease infection, and disease severity. CH NPs improved the antioxidant ability of treated plants, boosting both enzyme-based and non-enzyme-based defense systems against *R. solani* compared to untreated plants. CH NPs induced the transcription level of defense genes (APX, CAT, and SOD) in lucky bamboo-infected plants. Especially in CH NPs (50 mg/L) treated plants, which were increased by 1.8, 1.7, and 2.3-fold the gene expression level of APX, CAT, and SOD (defense gene) compared to control infected plants. CH NPs offer disease control insights, advanced research into agricultural nanomaterials, and use eco-friendly nano fungicides for sustainable agriculture.

Keywords: Chitosan Nanoparticles; *Rhizoctonia solani*; Lucky Bamboo; Root rot, ROS, Antioxidant Gene Expression

*Correspondence : **Mohamed A. Mahmoud**
E-mail: m.a.mahmoud75@gmail.com

Mohamed A. Mahmoud
https://orcid.org/0000-0003-3940-5753
Samy A. Almorsy
Hamada F.A. Ahmed
Abeer R. M. Abd El-Aziz
1-Plant Pathology Research Institute, Agricultural Research Center (ARC), Giza 12619, Egypt

INTRODUCTION

Dracaena sanderiana hort. ex. Mast. is classified within the Asparagaceae family and is frequently referred to as "lucky bamboo" (Damen *et al.*, 2018). This species represents a prominent ornamental plant extensively utilized for interior decoration across Middle Eastern nations and globally within commercial environments including shopping centers, corporate buildings, and educational institutions (Morsy and Elshahawy, 2016). The plant's significant stems from its straightforward cultivation requirements using only water with minimal maintenance needs, its association with beneficial energy properties, and its capacity to mitigate atmospheric and ecological contamination (Abdel-Rahman *et al.*, 2020). Regrettably, pathogenic soil-dwelling fungi responsible for root pathologies in cultivated plants typically persist extensively in soil environments when left undisturbed and protected beneath plant debris (Panth *et al.*, 2020). In 2019, research was undertaken examining root decay and stem base deterioration in *Dracaena sanderiana* specimens obtained from three Egyptian governorates. The average disease incidence rate was determined to be 36% (Abdel‑Rahman *et al.*, 2023). *R. solani* represents a highly damaging fungal pathogen impacting numerous ornamental

species, inducing root decay, stem base deterioration, and wilting globally (Aiello *et al.*, 2017, Jemai *et al.*, 2021, Rashed *et al.*, 2021). This pathogen can infect various ornamental plants, especially throughout cultivation and/or postharvest storage phases latently, remaining inactive for extended periods (Traversari *et al.*, 2021). Multiple regions, including the Pacific Northwest United States, Australia, Asia, and European areas regard Rhizoctonia root decay as a significant concern (Smiley, 1990). Current root decay disease control depends on chemical fungicides. Excessive fungicide usage results in soil health degradation, environmental contamination, reduced plant nutrient absorption efficiency, and pathogen resistance development (Pathak *et al.*, 2022). Therefore, focus must shift toward developing environmentally safe, biodegradable agricultural chemicals for secure and efficient crop application. Hence, identifying effective compounds with antifungal properties and positive plant growth effects remains essential. Utilizing nanotechnology in agricultural pathogen control proved advantageous for enhancing crop development and productivity while suppressing disease-causing organisms through nanoparticle absorption, which strengthens plant immunity against diseases and promotes agricultural growth (Worrall *et al.*, 2018). A multifunctional biopolymer characterized by its safe, compatible, and degradable properties, chitosan finds application in farming systems. It functions notably as an antimicrobial immune-modulating agent and crop development enhancer (Kong *et al.*, 2010, Xing *et al.*, 2015, Sathiyabama *et al.*, 2016). Current research demonstrates that chitosan-derived nanoparticles serve as effective stimulators of protective oxidative and defensive enzymatic responses (Chandra *et al.*, 2015). Chitosan nanoparticles (CH NPs) demonstrated potent antifungal efficacy against numerous aerial plant pathogenic fungi, including *Alternaria solani* and *Botrytis cinerea* (Sathiyabama *et al.*, 2014, De Vega *et al.*, 2021) and root-dwelling plant pathogenic fungi, including *Fusarium oxysporum* f. sp. *cicer* and *R. solani* (Rahman *et al.*, 2021). Gene expression analysis of CH NPs-treated specimens revealed that elevated defensive responses resulted from heightened activation of resistance-associated genes. These results confirmed the strengthened natural immunity of plants through chitosan components within nanoparticles (Chandra *et al.*, 2015). CH NPs have additionally served as nano-fertilizers for enhancing pathogen resistance across diverse plant-pathogen interactions, including root-dwelling pathogenic fungi (Ingle *et al.*, 2022).

Consequently, the goals of this investigation were to (1) characterize morphologically and molecularly the causative agent of root rot and basal stem rot disease in lucky bamboo specimens, (2) assess the antimicrobial properties of CH NPs against *R. solani* root rot disease under controlled laboratory and greenhouse environments (3) examine their capacity to trigger systemic resistance against root rot disease in lucky bamboo specimens under greenhouse and field environments and ultimately, (4) elucidate the resistance induction mechanism through regulatory and defensive gene expression analysis and defensive enzyme activity measurements.

MATERIALS AND METHODS

CH NPs source

CHNPs were obtained from Nanotechnology and Advanced Materials Central Laboratory (NAMCL), Regional Center for Food and Feed (RCFF), Agricultural Research Center (ARC), Giza 12619, Egypt with 99.9% purity.

Characterization of CH NPs

The synthesized CHNPs were verified using UV spectrophotometry (Unico UV-2100 spectrophotometer, Unico Instrument Co. Ltd, China). CH NPs were undergone characterization via transmission electron microscopy (TEM) (JEOL, JEM-1010, Boston, USA). TEM enabled morphological examination of both nanoparticle varieties. Fourier transform infrared (FTIR) spectrophotometry (Bruker tensor 27 IR with

KBr discs, Massachusetts, United States) was performed for functional group identification. CH NPs chemical functional groups were identified within 4000–400 cm-1 wavelength ranges.

Isolation and identification of the isolated fungal species

300 lucky bamboo plants displaying root and basal stem decay manifestations were collected from Alexandria, Beheira, and Giza governorates, Egypt, during the August–October 2023 timeframe. *R. solani* was isolated from diseased lucky bamboo tissues. Approximately 3 cm segments of lucky bamboo tissues displaying pathological symptoms were undergone thorough rinsing with distilled water. Initially, lucky bamboo tissues received complete cleaning with sterile distilled water (SDW). Subsequently, surface sterilization occurred using sodium hypochlorite (2%) solution for 3 minutes, followed by triple washing with SDW. Specimens were then dehydrated between dual layers of sterilized filter papers and cultured on potato dextrose agar (PDA) medium supplemented with 300 mg/L streptomycin sulphate, maintained at 26 °C for 7 days (El-kazzaz *et al.*, 2023). Resulting fungal colonies were undergone purification via single spore or hyphal tip methodology, the isolation of the fungi was carried out using morphological identification protocols (Booth, 1971, Barnett and Hunter 1998, Singh 2014).

Effect of CH NPs on the mycelial growth of *R. solani*

CH NPs underwent antifungal evaluation against *R. solani* isolate employing the poisoned food method (Vincent, 1947). Specifically, three selected concentrations of the biologically synthesized nanoparticles (25, 50, and 200 mg/L) were incorporated into PDA medium. Mycelial plugs (5 mm) were taken using a sterile cork borer and positioned at the center of PDA petri plates containing different concentrations of separate nanoparticles in triplicate and incubated at 25 °C for 7 days. Control PDA plates (without nanoparticles) served as reference. Subsequently, radial hyphal growth was quantified in each inoculated plate to evaluate the antimicrobial efficacy of different concentrations of each nanoparticle using the subsequent formula:

Inhibition of fungal growth (%) = [(A-a)/A] x 100

where A represents the mycelial growth of *R. solani* in the control plate and a represents the mycelial growth in the plate supplemented with different NPs.

Three replicate plates were used for each treatment and incubated until the control sample fully colonized the plate with R. solani growth.

Pathogenicity test and assessment efficacy of CH NPs on root rot, basal stem rot of lucky bamboo

Apparently healthy lucky bamboo specimens with uniform 70-cm length were obtained from a Giza nursery (Al-Mansouria region). These samples received thorough washing, disinfection (2% sodium hypochlorite for 2 min), and rinsing with sterile distilled water. For health assessment, samples were grown for 60 days in containers holding 300 ml autoclaved water under controlled laboratory conditions. Containers were fitted with sterilized cotton plugs preventing microbial contamination and moisture evaporation. Before use, each vessel was sterilized in dry heat oven for 2 hours at 180°C. Fungal inoculum of *R. solani* was developed according to (Büttner *et al.*, 2004). Particularly, *R. solani* was cultured in PDB (potato dextrose broth) using 250-ml Erlenmeyer flasks. Flasks were incubated at 20°C under dark conditions. Following 7 days, media became covered with mycelia. For pathogenicity testing, contents from five Erlenmeyer flasks were undergone homogenization and thorough maceration in metal blender to smooth liquid and adjusted to 1 litre using SDW. Ten ml suspension per plant served as liquid inoculum. The concentration of suspension was adjusted using the hemocytometer technique, viz 1×10^6 mycelial fragments/ml inoculum concentrations. Bamboo plants received distilled water washing then sterilization using 2% sodium hypochlorite (NaClO) for 2 min. Bamboo plants were positioned in 1 L sterile glassware (1

specimen/container) by immersing 5 cm basal stems with 300 ml SDW before implementation. Subsequently, bamboo specimens were prepared for CH NPs efficacy evaluation. Table (1) presents treatments utilized in this investigation. The experimental approach was randomized complete block design.

Table 1. Treatments used in this study.

Treatment Number	Treatment
T1 Control (negative)	The healthy bamboo plants submerged in sterile water for three hours and sowing in uninfested soil.
T2 Control (positive)	Soaking healthy bamboo plants in sterile water for three hours and sowing in infested soil with *R. solani*.
T3 (Infected + CH NPs soaking)	Soaking healthy bamboo plants in CH NPs (25 mg/L) for three hours and sowing in infested soil with *R. solani*.
T4 (Infected + CH NPs soaking)	Soaking healthy bamboo plants in CH NPs (50 mg/L) for three hours and sowing in infested soil with *R. solani*.
T5 (Infected + CH NPs soaking)	Soaking healthy bamboo plants soaking in CH NPs (100 mg/L) for three hours and sowing in infested soil with *R. solani*.

Disease Symptoms

Disease occurrence was evaluated 45 days post-cultivation following (Abdel‑Rahman, 2021). A disease severity scale (0–4) based on pathogen progression established by researchers was employed to quantify *R. solani* severity on root rot and basal stem rot.

The percentages of disease infection and disease severity were calculated by the following equations:

$$\text{Disease infection (\%)} = \frac{\text{No. of infected bamboo plants}}{\text{Total No. of bamboo (healthy and infected) of units assessed}} \times 100$$

$$\text{Disease severity (\%)} = \frac{\Sigma \text{ (Total No. of bamboo under scale} \times \text{scale degree)}}{\text{Scale degrees (4)} \times \text{Total No. of bamboo (infected) units assessed}} \times 100$$

Effect of CH NPs on root and shoot length, of *R. solani*-infected lucky bamboo plants

Biological impacts of different concentrations (25, 50, and 100 mg/L) of CH NPs were evaluated on shoot height and root length of lucky bamboo specimens. Shoot height was determined from lucky bamboo specimen base to apex in centimeters (cm); root length was determined from lucky bamboo specimen base to terminal root in cm.

Laboratory Studies

Antioxidant activity

The extraction procedure required weighing 10 g leaves and incorporating 100 mL methanol into samples. Samples were undergone maceration for 24 hours, filtration, and evaporation. Resulting extracts were preserved for subsequent analysis. Plant antioxidant activity utilizing 2,2-diphenyl-1-picrylhydrazyl (DPPH) assay was assessed using the method described by Katalinic *et al.*, (2004). Absorbance was recorded using spectrophotometer at 515 nm (Unico UV-2100 spectrophotometer, Unico Instrument Co. Ltd, China). Control was prepared with methanolic DPPH dilution. Calculations followed standard equation of mg ascorbic acid equivalent (AAE)/100 g.

Reactive Oxygen Species

Reactive oxygen species (ROS) were evaluated through quantification of superoxide anions $O2^{-}\bullet$ (µg g/1 FW), hydrogen peroxide (µmol g/1 FW, H2O2), and hydroxyl radicals (●OH, µmol g/1 FW) using established protocols of Yang *et al* (2011), Mukherjee and Choudhuri (1983), and Halliwell *et al.*, (1987) respectively.

Defense-Related Compounds

Total flavonoid content was colorimetrically evaluated following (Zou *et al.*, 2004). Flavonoid content absorbance was recorded at 510 nm. Phenolic compounds were quantified using Folin-Ciocalteu methodology following (Kofalvi *et al.*, 1995), employing gallic acid as standard reference. Total phenolics were reported as mg g/1 FW. Absorbance spectrum was recorded at 725 nm.

Antioxidant enzyme

Enzyme extraction

Leaf samples were ground in 50 mM K phosphate buffer, collected, centrifuged (10000 rpm), and stored at -20°C for enzymatic activity measurement

Superoxide dismutase (SOD)

SOD activity was quantified using methodology described by (Giannopolitis and Ries, 1977). Control sample contained a complete reaction mixture excluding enzyme extract. Absorbance was measured at 560 nm using UV–Vis spectrophotometer.

Catalase (CAT)

The CAT enzyme activity was determined using the procedure outlined by (Chance and Maehly 1955). Absorbance for CAT activity was assessed by monitoring the breakdown of H2O2 at 240 nm using UV–Vis spectrophotometer.

Ascorbate peroxidase (APX)

The APX enzyme activity was determined using the methodology provided by (Nakano and Asada 1981). Absorbance was recorded at 290 nm using UV–Vis spectrophotometer.

Gene expression analysis

RNA extraction and cDNA synthesis

A 100-mg bamboo leaf tissue sample was collected from CH NPs-treated and control plants, ground to fine powder using liquid nitrogen and homogenized in 1 mL TRIzol RNA isolation reagent (Invitrogen, USA). RNA extraction methodology followed by Ahmad *et al.*, (2017). One microgram RNA was utilized for cDNA synthesis using iScript cDNA synthesis kit (Bio-Rad, Hercules, CA, USA) following manufacturer's instructions.

Quantitative Real-time PCR (qRT-PCR)

qPCR primers targeting APX, CAT, and SOD genes were utilized for gene expression analysis, with actin gene (GU570135.2) serving as normalization control. These primers were documented by Ghodke *et al.*, (2020) Table (2). qRT-PCR reaction mixture contained SYBR Green Supermix (Bio-Rad, Hercules, CA, USA) following manufacturer's instructions. qPCR analyses were conducted using PCR equipment (real time analysis system, Rotor-Gene 6000, Qiagen, Hilden, Germany). Following qRT-PCR data acquisition, selected gene expression levels were computed using 2-ΔΔCt relative quantification method described by Livak *et al.*, (2001). All reactions were executed in triplicate.

Statistical Analysis

The obtained data underwent one-way ANOVA analysis following the protocol established by Gomez and Gomez (1980). Pairwise comparisons between treatment means utilized least significant difference (LSD) testing at 0.05 significance level.

RESULTS

Characterization of CH NPs

UV-Vis spectra

CH NPs optical characteristics were examined using UV-Visible spectroscopy as presented in Fig. (1). UV-Visible spectroscopy of CH NPs revealed broad absorption band with distinct intensity. The UV region absorption peak wavelength was detected at 310 nm (Fig.1).

FTIR spectroscopy

We examined CH NPs functional groups via FTIR spectroscopy. CH NPs FTIR spectra are presented in Fig. (2) and Table (3). CH NPs contained primary functional groups within their absorption bands, including hydroxyl group (OH) and carbonyl group (C=O). Table (3) provides all primary functional group specifications.

TEM

TEM analysis was carried out on the CH NPs to obtain the size and shape of the nanoparticles Fig. (3). The morphological analysis of the CH NPs showed that they were spherical, with some agglomerating small particles. SEM showed a nanoparticle size similar to that of TEM, ranging from 11.4 to 16.6 nm (Fig. 3).

Survey of root rot, basal stem rot on lucky bamboo

During August-October 2023 investigation period, the extensive examination for root and basal stem decay on lucky bamboo plants revealed typical manifestations in assessed sites including commercial establishments, florist shops, and cultivation facilities from different Egyptian regions (Alexandria, Beheira, and Giza

governorates). However, examined sites showed considerable differences in infection rates and pathological intensity (Table 4). According to Table 4 findings, average disease infection rate was maximum in samples obtained from Beheira (44.7%), followed by Alexandria (37.7%) and Giza (27.7%) governorates. Conversely, plant disease severity across three examined governorates ranged between 25.91 and 28.7%, with no significant variations among surveyed governorates Table (4).

Table 2. List of qRT-PCR primers used in this study

Primer Name	Primer Sequence	Product Length
CAT	5′ -CTCTCAAACCGAACCCAAAA-′ 3	149 bp
	5′ -GCCAGAACCTTCCATGTGTC-′ 3	
SOD	5′ -TTCCTCCAGCATTCCCAGTG-′ 3	228 bp
	5′ -ATGGCTTGACACATGGTGCT-′ 3	
AOX	5′ -TGATGTTTGTGCTGTCTTTCGG-′ 3	133 bp
	5′ -ACCGTGAAAGTGTTTGTGCT-′ 3	
WRKY70	5′-TGGAGAGTTCGCTGGTCAAA-′ 3	210 bp
	5′ -TACAGCCTCTGCGAGAAACG-′ 3	
NAC29	5′-ATAAAGCCATGTTCGGCGAC-′ 3	172 bp
	5′ -GCCTTTTTCACCCCGATGTT-′ 3	
Actin	5′ -CGATGAAGCACAATCCAAGA-3	138 bp
	5′ -TGTTCTTCAGGAGCAACACG-′ 3	

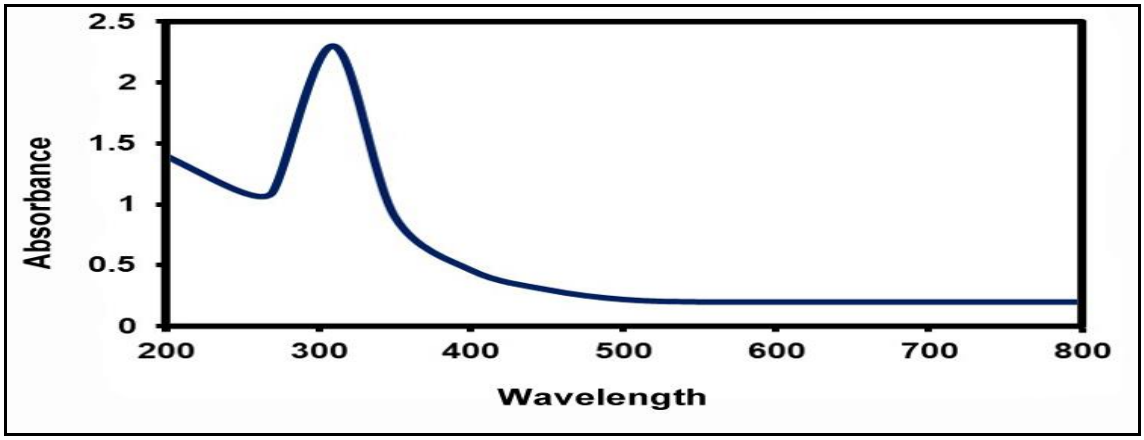

Fig. 1 UV-vis spectrum of CH NPs

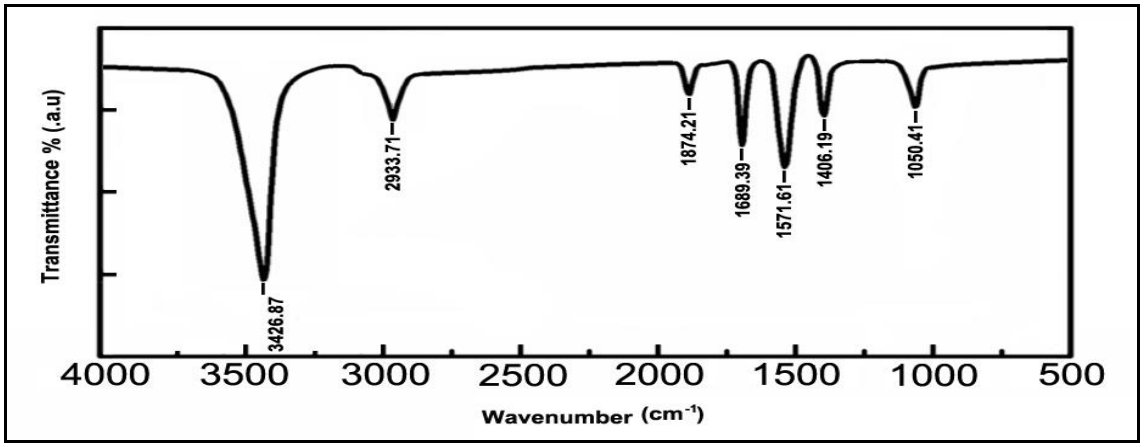

Fig. 2 FTIR spectra of CH NPs

Table 3. FTIR interpretation of compounds in CH NPs

S No.	Wave Number cm^{-1} Reference	Wave Number cm^{-1} CH NPs	Functional Group Assignment	Compounds Identified
1	3500-3300	3426.87	O-H stretch	Poly hydroxy compound
2	2800-2900	2933.71	Asymmetric stretching of –CH (CH2) vibration	Saturated aliphatic lipids compound
3	1800	1874.21	C–O and C–C stretching	aldehyde or ketone or organic acid or alkene compound
4	1600	1689.39	C=O stretching vibration, Ketone group	Ketone compound
5	1500	1571.61	NH2 bending vibration	Primary amides compound
6	1400	1406.19	C = N stretching in imines or oximes, or C-N stretching in aliphatic amines	amide III compound
7	1100-1000	1050.41	C-O stretch or C-N stretch	alcohols, phenols, ethers or esters compound,aromatic amines compound

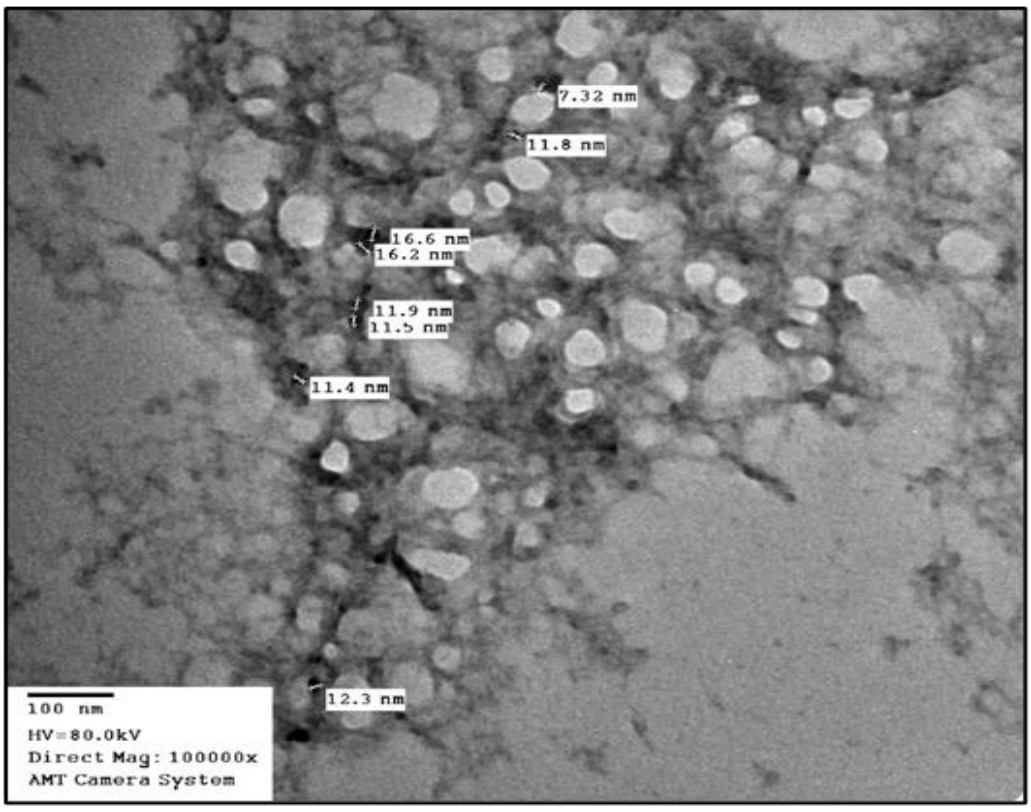

Fig.3 TEM image of CH NPs

Table 4. Occurrence of naturally disease infection and disease severity (%) of root rot and basal stem rot of lucky bamboo plants observed in surveyed locations in the three Egyptian governorates

Governorates	Total no. of surveyed plants	No. of infected plants	Disease infection (%)	Disease severity (%)
Alexandria	100	39	37.3[b]	25.3[b]
Beheira	100	44	44.7[a]	28.7[a]
Giza	100	28	27.7[c]	26.1[ab]
Means	100	37	35.6	26.7
L.S.D. at 0.05	-	-	2.83	2.70

*Values within the same column followed by a different letter (s) are significantly different at the 0.05 level of probability.

Fungi associated with root rot and basal stem rot disease in lucky bamboo plants

Isolation from diseased lucky bamboo specimens revealed six fungal species representing four distinct genera associated with root and basal stem decay symptoms Table (5). Among these pathogenic organisms, *R. solani* Kühn emerged as the predominant species within the collected fungal isolates. This pathogen accounted for 74.5% of all recovered specimens, while *Fusarium oxysporum* Schlecht and *F. solani* (Mart.) Sacc. demonstrated isolation rates of 7.2 and 6.5%, respectively.

Table 5. The mean frequency of fungal species recovered from diseased root rot and basal stem lucky bamboo rot after being surveyed from different locations in the three Egyptian governorates

The isolated fungi	No. of isolates			*F (%)
	Roots	Stems	Total	
A.alternata	0.0	5.0	5.0	3.3
A.niger	6.0	3.0	9.0	5.9
A.terreus	0.0	4.0	4.0	2.6
F.oxysporum	2.0	9.0	11.0	7.2
F. solani	3.0	7.0	10.0	6.5
R.solani	41.0	73.0	114.0	74.5
Total counts of fungal isolates	52.0	101.0	153.0	100.0

Confirmation the identification by GenBank database

These represented the morphological characteristics of the *R. solani* isolate (Fig. 4). The internal transcribed spacer (ITS) sequence of ribosomal DNA was employed to molecularly characterize the pathogenic organism of lucky bamboo root decay, basal stem decay disease. We used primers ITS1 and ITS5 to make 650-bp DNA products from a *R. solani* isolate that was amplified using PCR. Following identification, the *R. solani* isolate's ITS region was assigned an accession number (PQ046734) in the GenBank database. The isolated fungal strain's ITS sequence revealed 100% identity to the *R. solani* isolation sequence, which has the accession number (PQ046734).

In vitro antifungal activity of CH NPs on *R. solani* growth

The antimicrobial effectiveness of CH NPs against *R. solani* was assessed through radial growth inhibition assays (Figs. 5 and 6). These nanoparticles exhibited significant concentration-dependent fungistatic properties against *R. solani*. Elevated CH NPs concentrations produced wider zones of inhibition, while lower concentrations showed reduced effects. Treatment with CH NPs at three varying concentrations (20, 50, and 100 mg/L) markedly suppressed the radial expansion of *R. solani*. The maximum CH NPs concentration (100 mg/L) completely prevented hyphal development (100% growth inhibition) of *R. solani*. Implementation of CH NPs at these three concentrations (25, 50, and 100 mg/L) substantially decreased the radial expansion of *R. solani*.

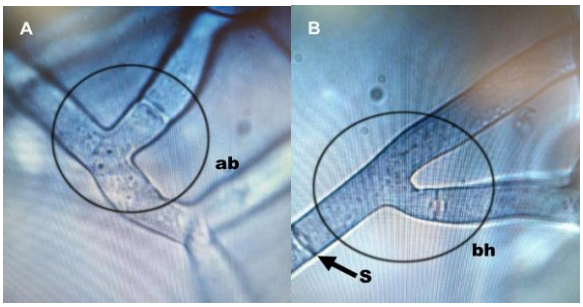

Fig.4 Microscopic characteristics of *R. solani* isolated from basal stems and roots of bamboo plants (X40): (A) microscopic traits of *R. solani* of the hyphal stage at a typical angle branching (ab); (B) numerous branching filaments of specialized hyphae composed of compact cells branching hyphae (bh) and septum (s).

Pathogenicity test and effectiveness of CH NPs against *R. solani* root rot infecting lucky bamboo plants

Lucky bamboo plants infected with *R. solani* showed disease symptoms 60 days later, including a rotting basal stem (RBS), discoloration at the basal stem (DBS), many black lesions on the stalk (BLS), discoloration at the stalk (DS), and finally plant death (Fig. 7). Because no disease symptoms appeared, the control treatments for lucky bamboo plants with CH NPs were very significant. At all concentrations of CH NPs, root rot caused by *R. solani* was much less common than in plants that had only been infected with the pathogen (74.5%). Also, a significant difference was observed in the disease symptoms of plants exposed to 25, 50, and 100 mg/L CH NPs compared to infected plants Fig. (7).

CH NPs enhanced the root and shoot length of lucky bamboo plants grown in soil with *R. solani*

Application of CH NPs to lucky bamboo plants markedly enhanced both root and shoot development in *R. solani*-challenged specimens (Fig. 8 A,B). Consequently, each evaluated CH NP concentration substantially promoted root and shoot elongation in both uninfected and *R. solani*-challenged plants.

Effect of CH NPs on the biochemical traits of lucky bamboo plants grown in soil with *R. solani*

Effect of CH NPs on Leaf antioxidant activity

Infection of lucky bamboo plants with *R. solani* led to a big increase in total antioxidant activity (TAA) when they were treated with different concentrations of CH NPs compared to the control plants. The infection increased the contents of TAA in the plants (Fig. 9) by about 1.7-fold, relative to the healthy plant when treated with 100 mg/L CH NPs.

The effect of CH NPs on ROS (oxidative stress) of lucky bamboo plants grown in soil with *R. solani*

Infection plants of lucky bamboo had higher reactive oxygen species values than healthy plants when CH NPs were applied at different concentrations (Fig. 10). Infected plants with *R. solani* had a lower accumulation of hydrogen peroxide (10.1% Fig. 10A), of superoxide anions (16.1%; Fig. 10B), and hydroxyl radicals (8.5%; Fig. 10C) than infected plants that were infected (control) treated with 25 mg/L CH NPs. CH NPs reduced ROS generation, indicating that they may alleviate oxidative stress and enhance the production of defense-related metabolites.

CH NPs induced the accumulation of defense-related compounds of lucky bamboo plants grown in soil with *R. solani*

The use of different levels of CH NPs in infected plants instigated the production of plant secondary metabolites. Exposure of plants to a concentration of various concentrations had a significant impact compared to other levels in stimulating the production of secondary metabolites (Fig. 11A, B). The presence of CH NPs at 100 mg/L in various concentrations increased the levels of flavonoids and total phenolics (Fig. 11), in the infected plants up to about 1.71-fold and 1.24-fold, respectively, compared to the control plants.

CH NPs induced the enzymatic antioxidant machinery of lucky bamboo plants grown in soil with *R. solani*

The antioxidant enzyme systems demonstrated notable responses to *R. solani* pathogen challenge in plants following various CH NPs concentration treatments. APX (Fig. 12A), CAT (Fig. 12B), and SOD (Fig. 12C) enzyme activities increased by 1.1-, 1.12, and 1.6-fold, respectively, compared to pathogen-challenged plants when applying CH NPs at 50mg/L. Notably, all enzyme activities remained equivalent to pathogen-infected plants under the combined influence of *R. solani* challenge while exceeding those of positive control plants.

Impact of CH NPs on antioxidant enzymes gene expression

The expression levels of APX, CAT, and SOD genes were evaluated by qRT-PCR in lucky bamboo leaves treated with different concentrations of CH NPs (Fig. 13). Defense-related gene expression was markedly enhanced following various CH NP concentration applications (Fig. 13). Elevated relative expression levels of APX,

CAT, and SOD genes determined through qRT-PCR analysis were detected in treated lucky bamboo specimens following application. The maximum expression level was found to be up-regulated at CH NPs (50 mg/L), 1.8-fold for APX, 1.7-fold for CAT, and 2.3-fold for SOD compared to the control infected level. It is clear that it was revealed that in the CH NPs-treated plants at 25 and 100 mg/L were up-regulated APX, CAT, and SOD compared to the control (infected) but not like 50 mg/L, which had highly significant gene expression.

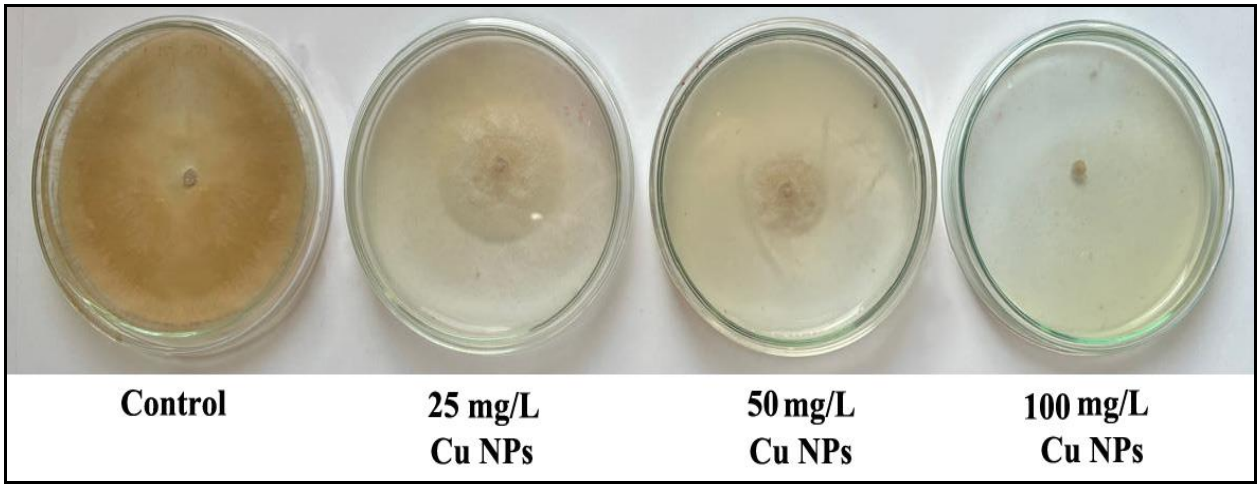

Fig. 5 Effect of CH NPs on the radial growth of *R. solani* (A) = control, (B) = CH NPs, 25 mg/L, (C) = Ch NPs, 50 mg/L, (D) = CH NPs 100 mg/L

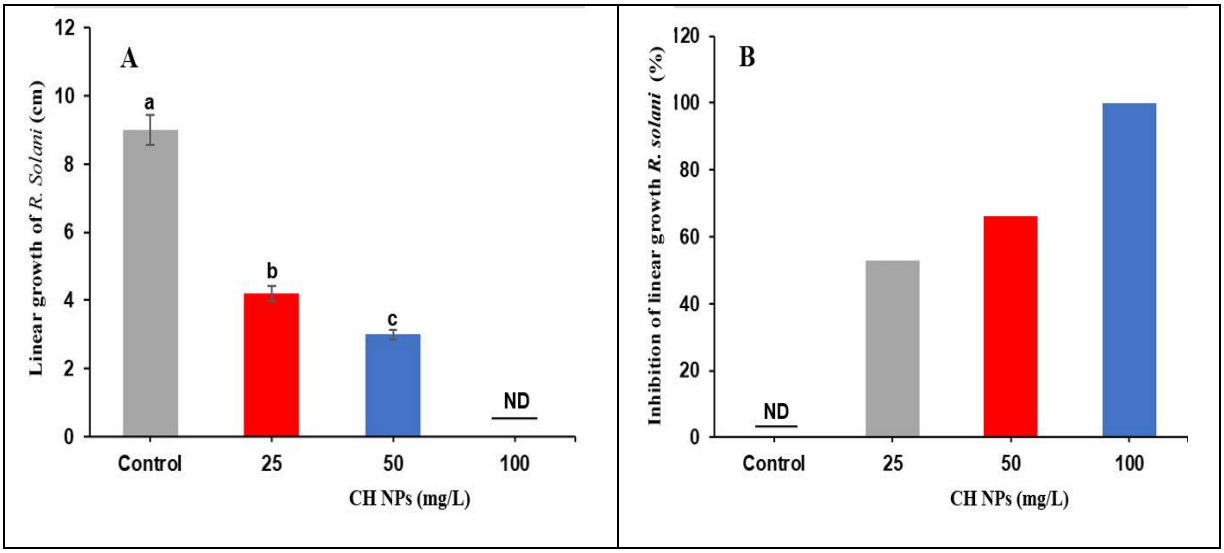

Fig. 6 *In vitro* antifungal activity of CH NPs against *R. solani*. (A) Linear growth (cm) of *R. solani* after the treatment with different concentrations of CH NPs NPs (0, 25, 50, and 100 mg/mL), The different alphabetic superscripts in the same column are significantly different ($p < 0.05$) based on Tukey's multiple comparison test.

DISCUSSION

UV-visible spectroscopy of CH NPs revealed a distinct absorption band, with peak absorption wavelength at 320 nm within the UV range. Our results align well with OH *et al*., (2019), El-Naggar *et al*., (2022). Based on FTIR analysis, CH NPs spectra displayed multiple peaks indicating functional groups presented in Table (3) and Fig. (2). Comparable research (OH *et al*., 2019) validated our FTIR results. TEM imaging offered comprehensive morphological information regarding CH NPs shape and size. Observations showed

that CH NPs exhibited nearly spherical morphology with relatively uniform particle distribution; no aggregation occurred (El-Naggar *et al*., 2022). Antimicrobial efficacy of CH NPs was examined against plant pathogenic fungi. CH NPs antimicrobial properties against certain plant pathogen, specifically *Fusarium oxysporum*, *Phytophthora capsici*, and *Gibberella fujikuori*, were investigated. In another study CH NPs demonstrated maximum growth inhibitory activity on *F. oxysporum* mycelial development (63.2%) followed by *P. capsici* (60.7%).

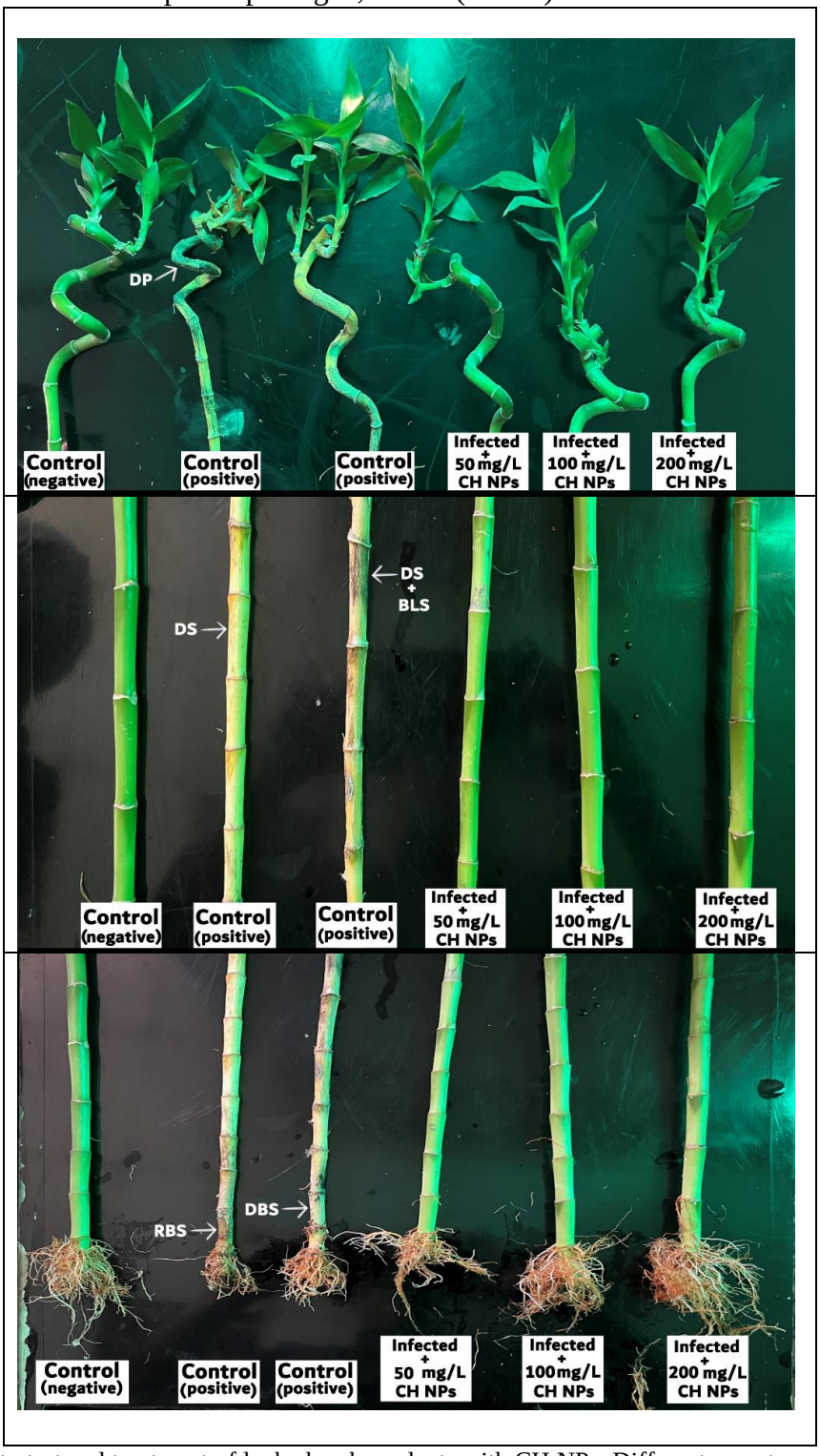

Fig. 7 Pathogenicity test and treatment of lucky bamboo plants with CH NPs. Different symptoms: (RBS) symptoms of the rotting basal stem of bamboo plants grown in soil infested *R. solani* (DBS) discoloration at the basal stem; (BLS) numerous black lesions on the stalk and spread to the entire stalk; (DS) discoloration at the stalk; (DP) dead plants 60 days after planting in infested soil.

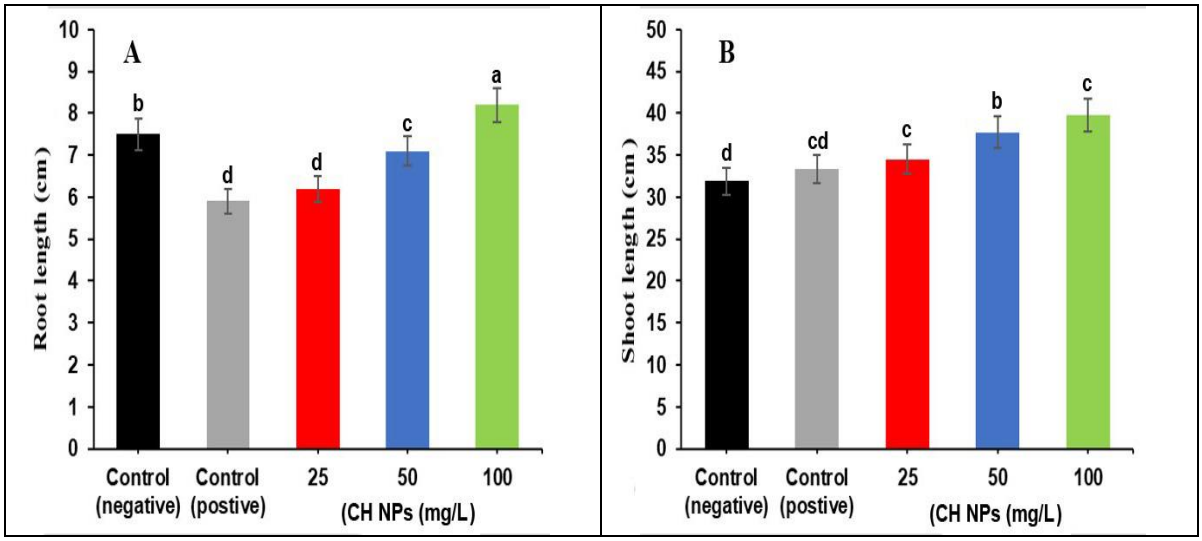

Fig. 8 Effect of CH NPs on vegetative traits of lucky bamboo plants under healthy and those grown in soil infested with *R. solani*. (A)root length (B) shoot length

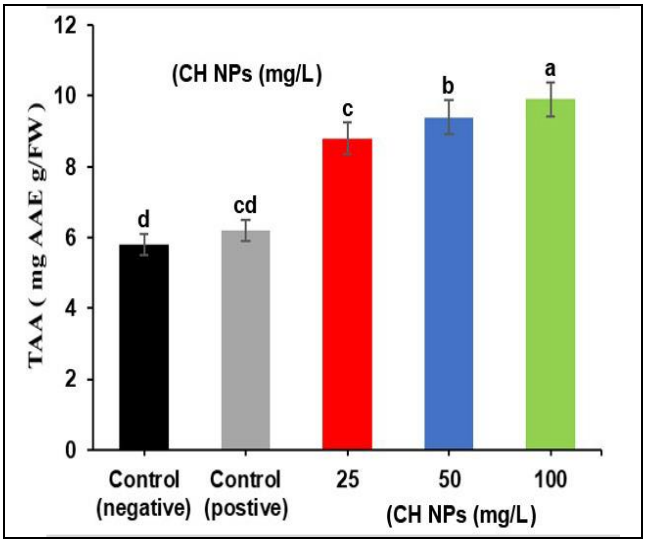

Fig. 9 Effect of CH NPs on total antioxidant activity of lucky bamboo plants under healthy and those grown in soil infested with *R. solani*.

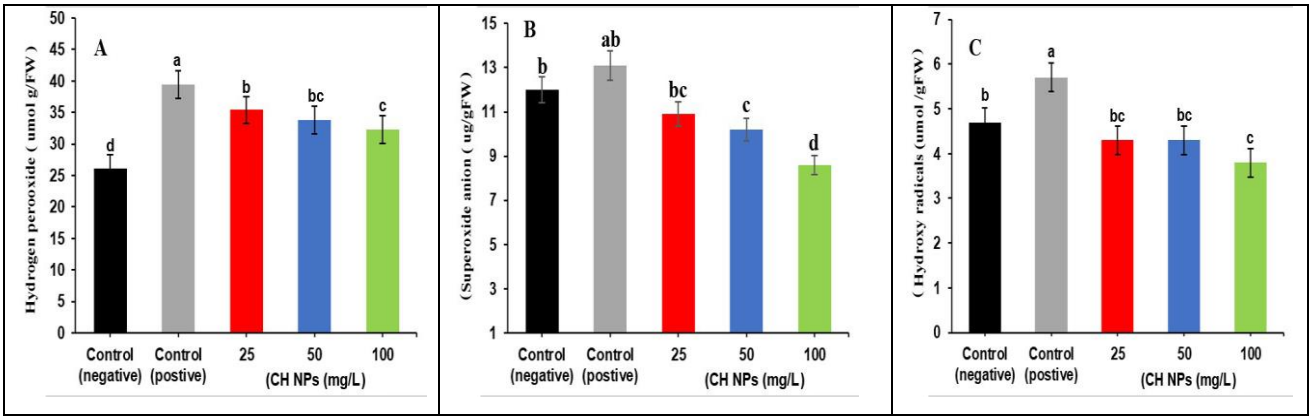

Fig. 10 Effect of CHNPs on oxidative stress-related compounds of lucky bamboo plants under healthy and those grown in soil infested with *R. solani*. (A) Hydrogen peroxide (µmol/g FW), (C) Superoxide anion (µg /g FW), (C) Hydroxyl radical (µmol /g FW)

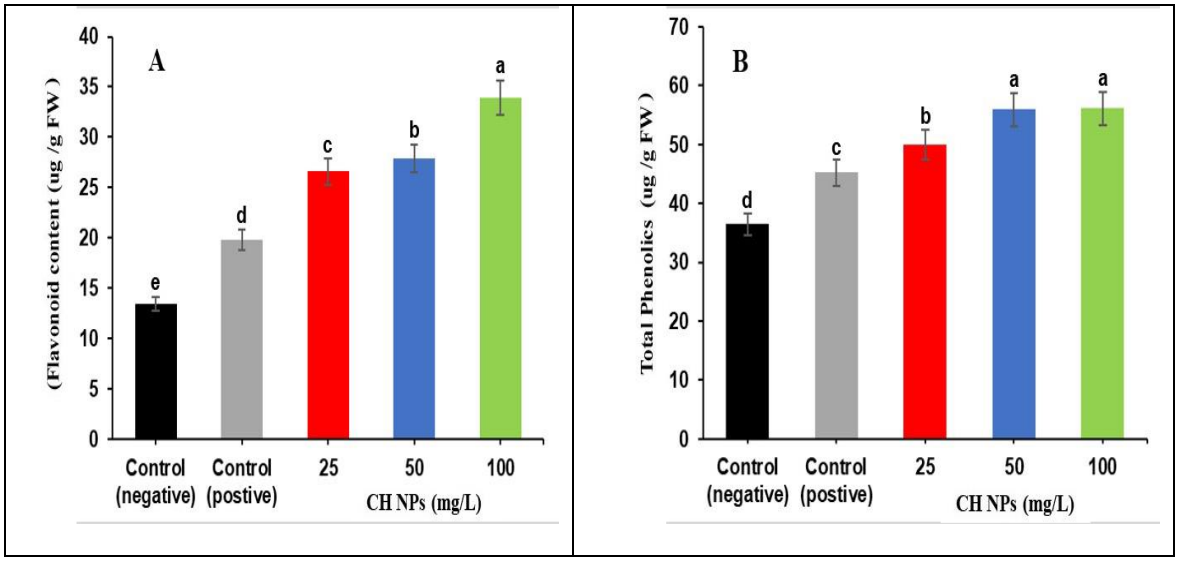

Fig. 11 Effect of CH NPs on defense-related compounds of lucky bamboo plants under healthy and those grown in soil infested with *R. solani*. (A) flavonoid content (B) total phenolics.

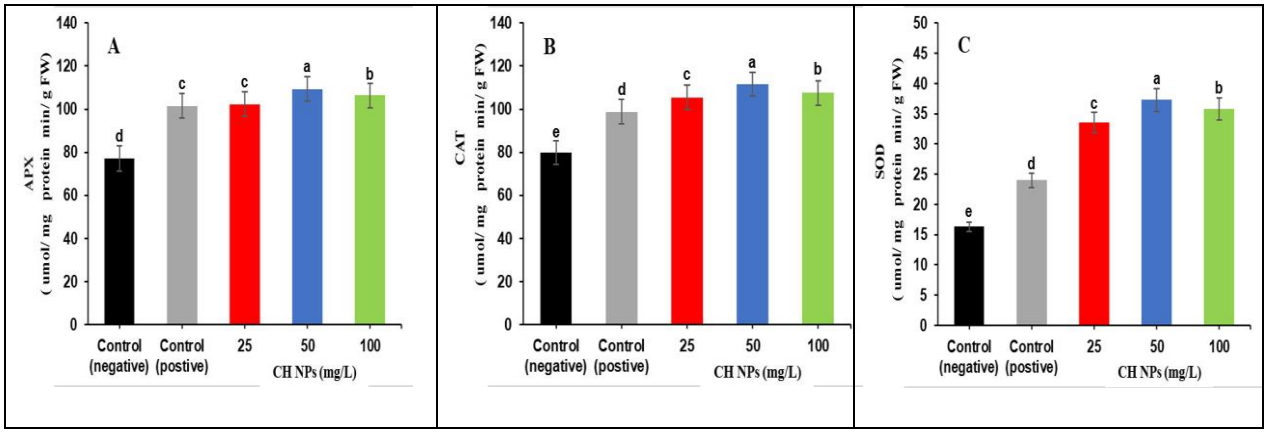

Fig. 12 Effect of CHNPs on enzymatic antioxidant machinery of lucky bamboo plants under healthy and those grown in soil infested with *R. solani*. (A) ascorbate peroxidase (APX), (B) catalase (CAT), (C) superoxide dismutase (SOD).

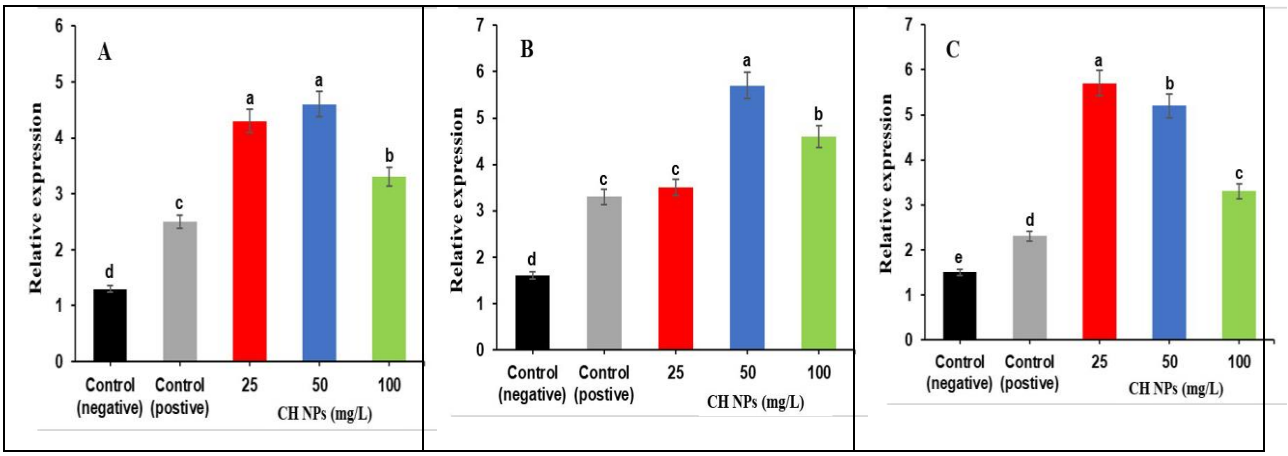

Fig. 13 Effect of CHNPs on expression of defense-related genes of lucky bamboo plants under healthy and those grown in soil infested with *R. solani*. (A) APX (B) CAT, and (C) SOD

These findings indicated CH NPs possess significant potential for safeguarding tomato cultivation from plant pathogenic fungi and warrant additional field evaluation (OH *et al*., 2019). In laboratory conditions, CH NPs biocontrol effectiveness against *R. solani* was examined using the detached leaf technique. Divya and his college proved that CH NPs are highly efficient in controlling *R. solani* with 93% disease reduction compared to 79% for chitosan. In greenhouse trials, CH NPs treatment achieved 75% disease incidence reduction, versus chemical fungicides with 30% disease reduction. Diseased leaf coverage was minimal for CH NPs at 16% while reaching 58% for chemical fungicide applications (Divya *et al.*, 2020). CH NPs, a safe biodegradable biopolymer, represent an effective biocontrol solution against *R. solani.* They function as potent plant immunity enhancers suitable as viable replacements for commercial chemical fungicides (Damen *et al*., 2018).

Egypt and other countries acknowledge lucky bamboo as an important indoor decorative plant. This plant holds significance due to its simple care requirements, low illumination tolerance, capacity to attract beneficial energy from surroundings through its aesthetic appeal, ability to neutralize atmospheric and environmental contaminants, etc. (Hugh *et al*., 2008, Damen *et al*., 2018). *R. solani* is among the most damaging fungal pathogens affecting numerous ornamental species including lucky bamboo, inducing root rot and basal stem rot, occasionally resulting in dieback of deteriorating roots and stems and potentially complete plant death (Abdel-Rahman *et al*., 2023).

Furthermore, numerous investigations have reported root and basal stem decay symptoms in introduced bamboo plants (Abdel-Rahman *et al*., 2023, Jemai *et al*., 2021). This study validated these findings through field surveys conducted between September–November 2023 across nurseries in different Egyptian regions, encompassing Alexandria, Beheira, and Giza. Disease incidence rates were maximum in Beheira (44.7%), subsequently Alexandria and Giza Governorates at 37.3% and 27.7%, respectively. Molecular identification of *R. solani*, pathogenic organism responsible for bamboo root decay disease was achieved utilizing ribosomal DNA ITS sequences. Through PCR amplification and ITS region primers, we amplified fungal isolate genomic DNA; the resulting PCR product measured 650 base pairs (bp) in length. BLAST analysis was subsequently employed to compare ITS DNA nucleotide sequence against NCBI's global database. *R. solani* displayed maximum similarity among fungal isolates. The nucleotide sequence was then submitted to GenBank database, registered, and assigned accession number PQ046734.

Fungal DNA ITS region serves as a commonly utilized molecular marker in fungal taxonomy, identification, classification, and phylogenetic research due to abundant reference sequences, elevated sequence variation, and conserved flanking regions, establishing it as a "fungal barcode" for individual genera and species of fungi (Bellemain *et al*., 2010). Regarding host plants, CH NPs application demonstrably enhances host plant resistance against phytopathogens and contributes significantly to host-pathogen interactions. Moreover, it reduces fungal disease severity and stimulates resistance against diverse plant pathogenic fungi causing root and foliar diseases (Boruah *et al*., 2021).

According to Lemire *et al*., (2013), five comprehensive mechanisms for nanoparticle antimicrobial activity have been proposed. (1) membrane transporter and nutrient uptake system disruption; (2) reactive oxygen species (ROS) generation damages multiple cellular organelles, including DNA, via oxidative stress and creates dysregulated cellular signaling; (3) toxic ion liberation causes membrane protein permeability alterations and denaturation; (4) genotoxicity and cellular death result from harmful ions released by nanoparticles, which significantly impact DNA; (5) reduced

energy generation, membrane oxidation, and pathogen protein oxidation prevent pathogens from performing metabolic functions. Precise biological mechanisms underlying potential silicon interactions with various biochemical pathways resulting in plant resistance against fungal pathogens remain unresolved. Silicon-mediated protective responses involve accelerated production of defensive metabolites, encompassing phenolic compounds, flavonoids, lignin, and phytoalexins, through primary and secondary biochemical pathways. CH NPs additionally boost defensive enzyme functions including phenylalanine ammonia-lyase (PAL), polyphenol oxidase (PPO), peroxidase (POX), and pathogenesis-related (PR) proteins (Dorjee *et al*., 2023). Remarkably, our findings showed that CH NPs application simultaneously activated multiple protective responses in treated lucky bamboo plantlets. These responses encompass (i) nanoparticles promoting ROS accumulation, inducing lipid peroxidation, nucleic acid deterioration, and protein oxidation (Fidalgo *et al*., 2013) and (ii) nanoparticles enhancing both enzymatic (POD, SOD, APX, CAT, and PPO) and non-enzymatic (phenolic compounds and flavonoids) antioxidant protective networks (Abdelrhim *et al*., 2021).

We examined the total phenolic alterations induced by CH NPs, a non-enzymatic antioxidant with crucial function in plant defense responses. Phenolics represent secondary metabolites containing aromatic rings that serve essential roles in plant defense through phytoanticipins and phytoalexins activity against pathogens (Dorjee *et al*., 2023). Consistent with earlier findings by Sarkar *et al*., (2022), who observed increased total phenolics from CH NPs in lentil and tomato, respectively, against *Alternaria* sp. Based on the work of Ji *et al*., (2022), which offers comprehensive insight into chitosan's oxidative stress reduction mechanisms, this understanding can improve chitosan utilization in agricultural plant protection. Nanoparticle cellular uptake triggers ROS formation, resulting in oxidative stress and nanotoxicity development, encompassing DNA damage, dysregulated cellular signaling, and apoptosis.

Overall, our results demonstrate that CH NPs enhance lucky bamboo defense systems against *R. solani* through enzymatic antioxidant defense machinery upregulation. CH NPs plant application resulted in elevated antioxidant enzyme activity including SOD, CAT, and APT in *Plasmopara halstedii*-infected sunflower plants versus healthy specimens (Nandeeshkumar *et al*, 2008).

CH NPs-induced resistance mechanisms are extensively researched across diverse host-pathogen interactions, confirming that CH NPs treatment invades pathogens via chemical and mechanical barrier biosynthesis while enhancing phytoalexin and defense enzyme synthesis (Falcón–Rodríguez *et al*., 2012).

SOD activity was markedly elevated in *Sclerospora graminicola*-infected pearl millet seedlings versus non-infected seedlings receiving CH NPs treatment. Additionally, SOD activity in infected CH NPs-treated seedlings was 2.32 times greater than non-infected seedlings. Identical patterns were observed regarding CAT activity in infected CH NPs (Siddaiah *et al*., 2018).

SOD expression progressively increased in *Sclerospora graminicola*-infected pearl millet seedlings receiving CH NPs treatment, with peak expression observed at 6 hours. SOD expression in CH NPs -treated seedlings was 3.47 times higher than untreated control seedlings. In identical research, CAT gene expression was progressively increased following pathogen inoculation, with transcript accumulation peaking at 6 hours. CAT gene expression in CH NPs -treated seedlings was 3.65-fold higher than untreated control seedlings (Siddaiah *et al*., 2018). Regarding SOD mRNA expression, it was upregulated 4.54-fold in *Fusarium andiyazi*-inoculated tomato plants treated with CH NPs versus control tomato plants. For CAT, it was upregulated 1.0-fold in pathogen-inoculated and CH NPs

-treated tomato plants versus control tomato plants. These results suggest that SOD and CAT could potentially safeguard plants against various oxidative stresses (Chun and Chandrasekara 2019).

CONCLUSION

In summary, CH NPs treatment decreased infection rates and inhibited *R. solani* development on lucky bamboo. Our results showed that CH NPs alleviate *R. solani* adverse impact on lucky bamboo plants by concurrently triggering a multi-tiered defense network encompassing at least three primary mechanisms. (i) CH NPs exhibit direct concentration-dependent fungistatic effects against *R. solani* vegetative development. (ii) CH NPs stimulate both enzymatic (APX, SOD, and CAT) and non-enzymatic (flavonoids and phenolics) antioxidant defense systems to counteract ROS destructive effects and preserve homeostasis within *R. solani*-infected specimens. (iii) Defense genes showed elevated expression levels in CH NPs -treated lucky bamboo specimens compared to untreated controls. Collectively, it is reasonable to suggest that CH NPs application represents a viable or environmentally-friendly strategy for protecting lucky bamboo specimens from root rot-inducing phytopathogenic fungi through their inhibitory effects against *R. solani*-caused infections.

AUTHOR CONTRIBUTIONS

Majority contribution for the whole article belongs to the author(s). The authors read and approved the final manuscript.

COMPETING INTERESTS

The authors declare that they have no competing interests. The contents of the manuscript have neither been published nor under consideration for publication elsewhere.

DISCLAIMER (ARTIFICIAL INTELLIGENCE)

The author (s) hereby declare that NO generative AI technologies such as Large Language Models (Chat GPT, COPILOT, etc.) and text-to-image generators have been used during the writing or editing of this manuscript.

STATEMENT AND ETHICS DECLARATIONS

The authors declare that they have no known competing financial interests or personal relationships that could have influenced the work reported in this article. Ethical approval was not required for this study.

REFERENCES

Abdel-Rahman, T.F.M., Abdel-Megeed, A. and Salem, M.Z.M, 2023. Characterization and control of *Rhizoctonia solani* affecting lucky bamboo (*Dracaena sanderiana* hort. ex. Mast.) using some bioagents. Scientific Reports, 13, 6691-6703.

Abdel-Rahman, T. F. M. 2021. Evaluation of the efficiency of some bio-fertilizers and different silicon sources for controlling bulb rot of *Lilium* Spp. In Egypt. J. Adv. Agric. Res. 26, 454–465.

Abdel-Rahman, T.F.M., El-Morsy, S. A. and Halawa, A. E. A. 2020. Occurrence of stem and leaf spots on lucky bamboo (*Dracaena sanderiana* hort. ex. mast.) plants in vase and its cure with safe means. Journal of Plant Protection and Pathology, 11,705–713.

Abdelrhim, A.S., Mazrou, Y.S.A., Nehela, Y., Atallah, O.O. El-Ashmony, R.M., and Dawood M.F.A, 2021. Silicon dioxide nanoparticles induce innate immune responses and activate antioxidant machinery in wheat against *Rhizoctonia solani*. Plants, 10, 1-19.

Aboul-Maaty, N.A. and Oraby H.A. 2019. Extraction of high-quality genomic DNA from different plant orders applying a modified CTAB-based method. Bulletin of the National Research Centre, 43, 25-43.

Ahmad, J., Baig, M.A., Ali, A.A., Al-Huqail, A., Ibrahim, M.M. and Qureshi, M.I. 2017. Comparative assessment of

four RNA extraction methods and modification to obtain high-quality RNA from *Parthenium hysterophorus* leaf. 3 Biotech, 7, 373-386.

Aiello, D., Guarnaccia, V., Formica, P.T., Hyakumachi, M. and Polizzi, G., 2017. Occurrence and characterisation of *Rhizoctonia* species causing diseases of ornamental plants in Italy. European Journal of Plant Pathology, 148, 967–982.

Al-Zaban, M.I., Alrokban, A.H. and Mahmoud, M.A. 2023. Development of a real-time PCR and multiplex PCR assay for the detection and identification of mycotoxigenic fungi in stored maize grains. Mycology, 14:227-238.

Barnett, H. and Hunter, B. 1998. Illustrated Genera of Imperfect Fungi 4th edn. (The American Phytopathological Society.

Bellemain, E., Carlsen, T. Brochmann, C. Coissac, E. Taberlet, P. and Kauserud, H. 2010. ITS as an environmental DNA barcode for fungi: an in silico approach reveals potential PCR biases. BMC Microbiol, 10, 189-202.

Boruah, S., and Dutta, P. 2021. Fungus mediated biogenic synthesis and characterization of chitosan nanoparticles and its combine effect with *Trichoderma asperellum* against *Fusarium oxysporum*, *Sclerotium rolfsii* and *Rhizoctonia solani*. Indian Phyto-pathology, 74, 81–93.

Büttner, G., Pfähler, B. and Märländer, B. 2004. Greenhouse and field techniques for testing sugar beet for resistance to Rhizoctonia root and crown rot. Plant Breeding, 123, 158–166.

Chance, B. and Maehly, A.C. 1955. The assay of catalases and peroxidases, Methods in enzymology, 764–775.

Chandra, S., Chakraborty, N., Dasgupta, A., Sarkar, J., Panda, K. and Acharya, K. 2015. Chitosan nanoparticles: A positive modulator of innate immune responses in plants. Scientific Reports, 165, 15195-15211.

Chun, S.C. and Chandrasekara M. 2019. Chitosan and chitosan nanoparticles induced expression of pathogenesis-related proteins genes enhances biotic stress tolerance in tomato. International Journal of Biological Macromolecules, 125, 948-954.

Damen, T., van der Burg, W., Wiland-Szymańska, J. and Sosef, M. 2018. Taxonomic novelties in African Dracaena (Dracaenaceae). Blumea, 63, 31–53.

De Vega, D., Holden, N., Hedley, P.E., Morris, J., Luna, E. and Newton A., 2021. Chitosan primes plant defence mechanisms against *Botrytis cinerea*, including expression of Avr9/Cf-9 rapidly elicited genes. Plant, Cell & Environment, 44, 290–303.

Divya, K.M., Thampi, Vijayan, S. Varghese, S. and Jisha, M.S. 2020. Induction of defence response in *Oryza sativa* L. against *Rhizoctonia solani* Kühn by chitosan nanoparticles. Microbial Pathogenesis, 149, 2020-104525.

Dorjee, L., Gogoi, R., Kamil, D., Kumar, R., Mondal, T.K., Pattanayak S. and Gurung, B. 2023. Essential oil-grafted copper nanoparticles as a potential next-generation fungicide for holistic disease management in maize. Frontiers in Microbiology, 14, 1-26.

El-kazzaz, M.K., Ghoneim, K.E., Agha, M.K.M., Helmy, A., Behiry, S.I., Abdelkhalek, A. Saleem, M.H., Al-Askar, A.A., Arishi, A.A. and Elsharkawy, M.M. Suppression of pepper root rot and wilt diseases caused by *Rhizoctonia solani* and *Fusarium oxysporum*. Life, 12, 587-599.

El-Naggar, N.E., Shiha, A.M., Mahrous, H. and Mohammed, A.A.B. 2022. Green synthesis of chitosan nanoparticles, optimization, characterization and antibacterial efficacy against multi drug resistant biofilm-forming

Acinetobacter baumannii. Scientific Reports, 12, 19869-19883.

Falcón–Rodríguez, A.B., Wégria, G. and Cabrera, J.C. 2012. Exploiting plant innate immunity to protect crops against biotic stress: chitosaccharides as natural and suitable candidates for this purpose. In: Ali, R. Bandani (Eds) New perspectives in plant protection. InTech. Rikeka, Coratia 7, 39–166.

Fidalgo, F.M., Azenha, A., Silva, F., Sousa, A., Santiago, A., Ferraz, P. and Teixeira. J. 2013. Copper-induced stress in *Solanum nigrum* L. and antioxidant defence system responses, Food and Energy Security, 2, 70–80.

Ghodke, P., Khandagale, K., Thangasamy, A., Kulkarni, A., Narwade, N. Shirsat, D. Randive, P., Roylawar, P., Singh, I., Gawande, S.J. and Mahajan, V. 2020. Comparative transcriptome analyses in contrasting onion (*Allium cepa* L.) genotypes for drought stress. PLoS One 15, 0237457-0237467.

Giannopolitis, C.N. and Ries, S.K. 1977. Superoxide dismutases: I. Occurrence in higher plants. Plant Physiology, 59, 309–314.

Gomez A.K. and Gomez, 1980. Statistical Procedures For Agriculture Research 2 nd Ed. John Wiley & sons New Youk, 680 PP.

Halliwell, B., Gutteridge, J.M.C. and Aruoma, O.I. 1987. The deoxyribose method: A simple "test-tube" assay for determination of rate constants for reactions of hydroxyl radicals. Analytical Biochemistry, 165, 215–219.

Hugh, T., Tan, W. and Giam. X. 2008. Plant Magic: Auspicious and Inauspicious Plants from Around the World, in: Marshall Cavendish Editions, 2008, ISBN 9789812614278, p. 62.

Ingle, P.U., Shende, S.S., Shingote, P.R., Mishra, S.S., Sarda, V., Wasule, D.L., Rajput V.D., Minkina, T., Rai, M., Sushkova, S., Mandzhieva, S. and Gade A. 2022. Chitosan nanoparticles (ChNPs): A versatile growth promoter in modern agricultural production. Heliyon, 8:11893.

Jemai, N., Gargouri, S., Hemissi, I., Mahmoud, K., Ksouri, M. and Jemmali A. 2021. *Rhizoctonia solani* affecting micropropagated Garnem (*Prunus amygdalus* x *Prunus persica*) rootstock - characterization and biocontrol with Rhizobia. Journal of Plant Pathology, 103, 207–215.

Ji, H., Wang, J., Chen, F., Fan, N., Wang, X., Xiao, Z. and Wang, Z. 2022. Meta-analysis of chitosan-mediated effects on plant defense against oxidative stress. Science of The Total Environment, 85, 158212-15822.

Katalinic, V., Milos, M., Kulisic T., and Jukic, M., 2006. Screening of 70 medicinal plant extracts for antioxidant capacity and total phenols. Food Chemistry, 94, 550–557.

Kofalvi, S.A and Nassuth, A. 1995. Influence of wheat streak mosaic virus infection on phenylpropanoid metabolism and the accumulation of phenolics and lignin in wheat. Physiological and Molecular Plant Pathology, 47, 365–377.

Kong, M. Chen X.G., Xing K. and Park, H.J., 2010. Antimicrobial properties of chitosan and mode of action: a state-of-the-art review. International Journal of Food Microbiology,144, 51–63.

Lemire, J.A., Harrison, J.J. and Turner, R.J. 2013. Antimicrobial activity of metals: mechanisms, molecular targets and applications. Nature Reviews Microbiology, 11, 371–384.

Livak, K.J. and Schmittgen T.D. 2001. Analysis of relative gene expression data using real-time quantitative PCR and the $2^{-\Delta\Delta CT}$ method. Methods, 25, 402–408.

Malandrakis, A.A., Kavroulakis N. and Chrysikopoulos C.V., 2019. Use of copper, silver and zinc nanoparticles against foliar and soil-borne plant pathogens. Science of The Total Environment, 670, 292-299.

Morsy, A.A. and Elshahawy, I.E. 2016. Anthracnose of lucky bamboo *Dracaena sanderiana* caused by the fungus *Colletotrichum dracaenophilum* in Egypt. Journal of Advanced Research, 7, 327–335.

Mukherjee, S.P. and Choudhuri, M.A. 1983. Implications of water stress-induced changes in the levels of endogenous ascorbic acid and hydrogen peroxide in Vigna seedlings. Physiologia Plantarum, 58, 166–170.

Nakano, Y. and Asada, K. 1981. Hydrogen peroxide is scavenged by ascorbate-specific peroxidase in spinach chloroplasts. Plant and Cell Physiology, 22, 867–880.

Nandeeshkumar, P., Sudisha, J. and Kini K. Ramachandra, H.S. Prakash, S.R. Niranjana, Shetty H. Shekar, 2008. Chitosan induced resistance to downy mildew in sunflower caused by *Plasmopara halstedii*. Physiological and Molecular Plant Pathology, 72, 188–194.

OH, J.W., Chun, S.C. and Chandrasekaran, M. 2019. Preparation and in vitro characterization of chitosan nanoparticles and their broad-spectrum antifungal action compared to antibacterial activities against phytopathogens of tomato. Agronomy 9, 21-37.

Panth, M., Hassler S.C. and Baysal-Gurel F. 2020. Methods for management of soilborne diseases in crop production. Agriculture, 10,16-39. doi:10.3390/agriculture10010016.

Pathak, V.M., Verma, V.K., Rawat, B.S., Kaur, B., Babu, N., Sharma, A., Dewali, S., Yadav, M., Kumari, R., Singh, S., Mohapatra, A., Pandey, V., Rana N. and J.M. Cunill, 2022. Current status of pesticide effects on environment, human health and it's eco-friendly management as bioremediation: A comprehensive review. Frontiers in Microbiology, 13, 962619-962631.

Rahman, M.A., Jannat, R., Akanda, A.M., Khan, M.A.R. and Rubayet M.T. 2021. Role of chitosan in disease suppression, growth and yield of carrot. European Journal of Agriculture and Food Sciences, 3, 34–40.

Rashed, O., Abdullah, S.N.A., Alsultan W., Misawa T., Khairulmazmi, A. and Kutawa, A. 2021. Characterization of inter and intra anastomosis group of *Rhizoctonia* spp. isolated from different crops in Peninsular Malaysia. Tropical Plant Pathology, 46, 422–434.

Sarkar, A., Chakraborty, N., and Acharya, K. 2022. Chitosan nanoparticles mitigate Alternaria leaf spot disease of chilli in nitric oxide-dependent way. Plant Physiol. Biochem. 180, 64–73.

Sathiyabama, M. and Manikandan A. 2016. Chitosan nanoparticle induced defense responses in fingermillet plants against blast disease caused by *Pyricularia grisea* (Cke.) Sacc. Carbohydrate Polymers, 154, 241–246.

Sathiyabama, M., Akila, G. and Charles R.E. 2014. Chitosan-induced defence responses in tomato plants against early blight disease caused by *Alternaria solani* (Ellis and Martin) Sorauer. Archives of Phytopathology and Plant Protection, 47,1963–1973.

Siddaiah, C.N., Prasanth, K.V.H., Satyanarayana, N.R., Mudili, V., Gupta, V.K., Kalagatur, N.K. Satyavati, T. Dai, X.F. Chen, J.Y. Mocan, A. Singh, B.P. Srivastava, R.K. 2018. Chitosan nanoparticles having higher degree of acetylation induce resistance against pearl millet downy mildew through nitric oxide generation. Scientific Reports, 1, 2485-2499.

Smiley, R.W.1990. Impact of fungicide seed treatments on *Rhizoctonia* root rot, take-all, eyespot, and growth of winter wheat. Plant Disease, 74,782-790.

Traversari, S., Cacini, S., Galieni A., Nesi B., Nicastro N. and Pane C. 2021. Precision agriculture digital technologies for sustainable fungal disease management of ornamental plants. Sustainability, 13, 3707-3717.

Vincent J.M. 1947. Distortion of fungal hyphae in the presence of certain inhibitors. Nature, 159, 850-861.

White, T.J., Bruns, T.D., Lee, S.B. and Taylor J.W. 1990. Amplification and Direct Sequencing of Fungal Ribosomal RNA Genes for Phylogenetics. In: Innis, M.A.

Worrall, E.A., Hamid, A. Mody K.T., Mitter N. and Pappu H.R. 2018. Nanotechnology for plant disease management. Agronomy, 8, 285-299.

Xing, K., Zhu, X., Peng, X. and Qin S., 2015. Chitosan antimicrobial and eliciting properties for pest control in agriculture: a review. Agronomy for Sustainable Development, 35, 569–588.

Yang, H., Wu, F. and Cheng J. 2011. Reduced chilling injury in cucumber by nitric oxide and the antioxidant response. Food Chemistry. 127, 1237–1242.

Zou, Y., Lu, Y. and Wei, D. 2004. Antioxidant activity of a flavonoid-rich extract of *Hypericum perforatum* L. in vitro. Journal of Agricultural and Food Chemistry, 52, 5032–5039.